# Biaxial Loading of a Textile Ribbons Structure for an Inflatable Module of Space Habitats

**C. Monticelli [1], V. Carvelli [1ID], Z. Fan [1], D. Valletti [2], M. Nebiolo [3], A. Messidoro [4]**

Abstract The aim of the experimental campaign was to assess and observe the biaxial tensile mechanical response of a rib-bons structure as part of an inflatable module of space habitats. The structure consists of orthogonal Zylon™ and Kevlar™ ribbons connected at crossover by Nylon thread seams. A clamping system was designed and manufactured to reproduce the biaxial loading condition supposed in the inflatable module application. The tests were assisted by a digital image correla-tion system. The images post-processing allowed the observa-tion and measurement of the full field strain of the different connection schemes. The results of the tests show the excellent mechanical performance of the ribbons structure at the maxi-mum biaxial load level without visible damage.

Keywords Inflatable module . Ribbon structure . Biaxial mechanical behaviour . Digital image correlation

## Introduction

Conventional space habitat modules for orbital and planetary locations are based on metallic structures having limitations related to volume and weight that can be launched to orbit. Future manned space habitat, characterized by extended mis-sion periods, would require larger available space for astro-nauts and consequently greater mass to be delivered in orbit.

Inflatable manned modules technology, as underlined by Thales Alenia Space-Italia (TAS-I) [1, 2], offer the possibility to deploy on-orbit large structures and have high habitable volumes in spite of a reduced volume at launch due to their high packaging capability and reduced mass using lightweight materials.

Received: 15 February 2016
Accepted: 12 August 2016
Published online: 19 August 2016

✉ V. Carvelli
valter.carvelli@polimi.it

[1] Department of Architecture, Built Environment and Construction Engineering, Politecnico di Milano, Piazza Leonardo da Vinci 32, 20133 Milan, Italy

[2] AKKA, Via Torino 166, 10093 Collegno, TO, Italy

[3] Thales Alenia Space – Italia, Strada Antica di Collegno 253, 10146 Torino, Italy

[4] Space & Technology Division, Aero Sekur S.p.A., Via Bianco di Barbania 16, 10072 Caselle T.se, TO, Italy

As preliminary investigated in the ESA IMOD project [3–5] the inflatable module technology for space habitats re-lies on a combination of flexible fabric and polymeric layers combined with rigid or foldable metallic elements and bulk-heads to drive packaging and deployment operations and to provide internal interfaces for secondary structures (Fig. 1(a)).

Generally the flexible inflatable part is composed of five main functional layers (see Fig. 1(b)) [6]:

- Internal Barrier
- Air Containment Bladder
- Structural Restraint
- Micro Meteoroids & Orbital Debris (MMOD) Protection
- Multi-layer Insulation (MLI)

As the open and orbital space has no atmosphere, as well as the Moon (apart from some very tenuous gases being “outgassed” from the surface), any habitat would need to be pressurized to simulate the terrestrial atmosphere (to approx-imately 1 atm or 101,325 Pa) and atmospheric gas quantities. Due to the high forces acting outwards (by the maintained gas pressure), structural integrity of an inflatable has to be insured.

In the inflatable module layout, the Structural Restraint layer is the flexible layer aimed to sustain the load derived from the pressure gradient between the internal surface of

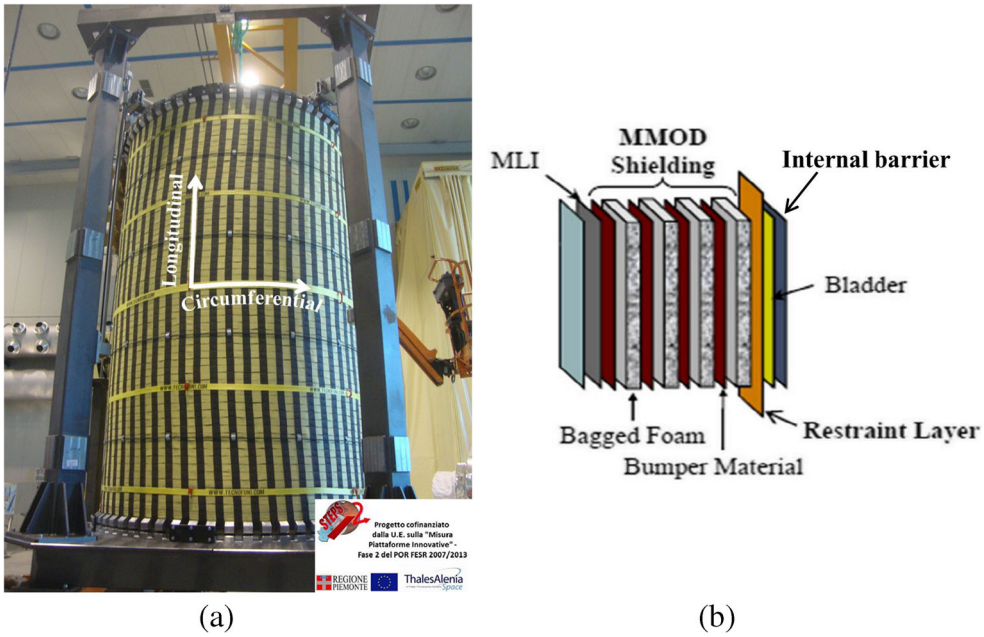


**Fig. 1** (**a**) Prototype of the inflatable module structural restraint. (**b**) Functional layers of the flexible inflatable part

the module (1 atm with habitable conditions for the astronauts) and the external surface of the module (0 atm corresponding to the open space vacuum).

In the development of the Structural Restraint for the inflatable module technology for orbital and planetary space habitats, one of the most significant and crucial loading condition is the biaxial tension of the Structural Restraint layer. Therefore, one of the important understandings in the design phase of the inflatable module is the biaxial tensile behaviour of the Structural Restraint layer and accurate experimental testing and modelling are required. This is the main object of the present study: the experimental investigation of the biaxial tensile behaviour of a representative breadboard (B/B) segment of the Structural Restraint layer.

The considered restraint B/B segment, made of ribbons as row materials and seams for the joints, fully replicates the Structural Restraint layer as in the real complete inflatable module.

The experimental investigation detailed in this paper considers the restraint B/B segment to assess the quasi-static tensile biaxial behaviour as in real loading condition. The biaxial tensile loading was applied with an available mechanical device assuming the load ratio in the two principal directions previously defined according the design requirements. One of the main aims of the investigation was the performance of the ribbons connection at the cross over with different seams. The tests were assisted by a digital image correlation system. The images post-processing allowed the calculation of the full field strain, on the external surface of the sample during loading, using commercial software. The relevant mechanical performance of the restraint B/B samples is here detailed considering load vs displacement diagrams of each actuator; maps of the strain components in the two principal directions.

## Samples and Experimental Setups

The tensile biaxial mechanical behaviour of perpendicular connections between Zylon™ and Kevlar™ ribbons were first investigated. One type is a structural sewing (high load bearing, named in the following S2), the other is a non-structural (low load bearing, named in the following S4). Specimens for each seam were manufactured with 49 mm wide Zylon ribbons and 45 mm wide Kevlar ribbons. Moreover, the same ribbons were adopted to reproduce a restraint B/B of the inflatable module, to assess the biaxial response of the assembly.

### Samples Features

#### *Materials*

The Zylon material selected for the longitudinal assembly is a 49 mm weave ribbon coated with Viton™ elastomer [7] in order to protect the fibres from UV degradation. It is supplied by SABELT S.p.A. and appositely modified for the application from an available commercial product, used as for automotive safety belts, in order to meet the tensile strength requirement. Table 1 lists the measured main properties of the Zylon ribbon. Figure 2 shows a typical force-elongation curve of the Zylon ribbon (elongation was measured by an extensometer having gage length of 85 mm).

The Kevlar material, selected for the hoop assembly, is a 44 mm weave ribbon. Differently from the longitudinal

**Table 1** Properties of 100 % PBO-Zylon Viton™ coated ribbon

| | |
|---|---|
| Unloaded | Width = 49.5 mm |
| | Thickness = 0.93 mm |
| | Linear Density = 34.2 g/m |
| At 10 kN | Width = 42.9 mm |
| | Thickness = 1.05 mm |
| Characteristic tensile strength | Nominal: 54.1 kN |
| | After abrasion: 53.9 kN |
| | After abrasion and UV: 46.9 kN (degradation: 13.3 %) |

**Table 2** Properties of 100 % Kevlar™ ribbon

| | |
|---|---|
| Unloaded | Width = 44 mm |
| | Thickness = 2.36 mm |
| | Linear Density = 76.7 g/m |
| At 10 kN | Width = 43.6 mm |
| | Thickness = 2.32 mm |
| Characteristic tensile strength | Nominal: 92.5 kN |
| | After UV: 67.7 kN (degradation: 26,7 %) |

ribbon, it is not coated for UV protection. It is thicker and softer than the corresponding longitudinal one. Table 2 lists the measured main properties of the Kevlar ribbon. A typical force-elongation curve of the Kevlar ribbon is depicted in Fig. 3.

*Seams and restraint B/B*

The knitted ribbons were connected perpendicularly by seams with Nylon thread in two different configurations: one high load bearing (S2) and the other low load bearing mainly adopted for stability of the connection (S4) (see Fig. 4).

The S4 seam connects two orthogonal ribbons with Nylon Zwibond 8 thread (100 % Nylon 6.6 bonded Nm. 8 black). This simplified pattern was adopted for keeping the position between longitudinal and circumferential ribbons (see Fig. 1(a)). This seam pattern has 103 stitches.

The S2 consists of 3 consecutive seams, labelled 'Ferrari', with longitudinal ribbon and Nylon Zwibon 8 thread (100 % Nylon 6.6 bonded Nm. 8 black), see Fig. 4. S2 connects two overlap Zylon ribbons and one orthogonal Kevlar ribbon in between and it is also used as closure of loops of Kevlar ribbons. The S2 seam consists of 303 stitches. Table 3 summarised the main parameters of the two seams.

Two types of specimens were considered for biaxial characterization: cruciform specimens consisting of orthogonal ribbons and a specimen consisting of a set of ribbons connected to each other (Restraint B/B) representing the segment of the structural restraint, one of the five layers of the inflatable module of space habitat.

The cruciform specimens were intended for testing the biaxial response of the two seam connections (Fig. 4). The specimens with seam S4 had free length of 300 mm in both directions and a connected surface of 43 × 48 mm$^2$. The specimens with seam S2 had free length of 265 mm in the direction of the Kevlar ribbon and of 100 mm in the direction of the Zylon ribbon, the crossover surface was 43 × 48 mm$^2$.

The specimen representing the Restraint B/B of the inflatable module had 4 Kevlar and 4 Zylon ribbons cross connected by seams (see the sketch in Fig. 5). The dimensions of the specimen are: 831 mm in the Kevlar and 343 mm in the Zylon direction, respectively. The central part, including all connections, was about 350 × 200 mm$^2$. The position and the type of seams in the specimen are detailed in Fig. 5. S4 seam connects

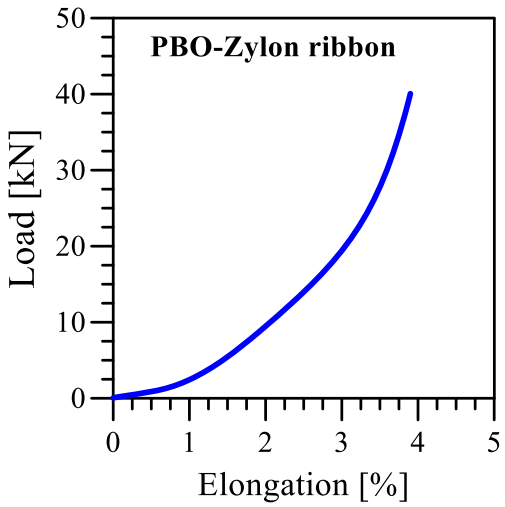


**Fig. 2** Typical force-elongation diagram of the 100 % PBO-Zylon VITON coated ribbon

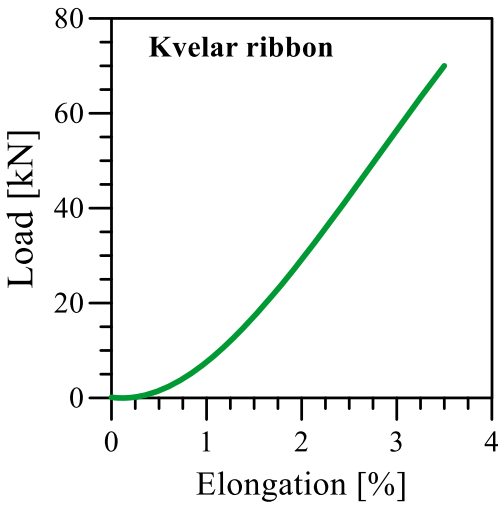


**Fig. 3** Typical force-elongation diagram of the 100 % Kevlar ribbon

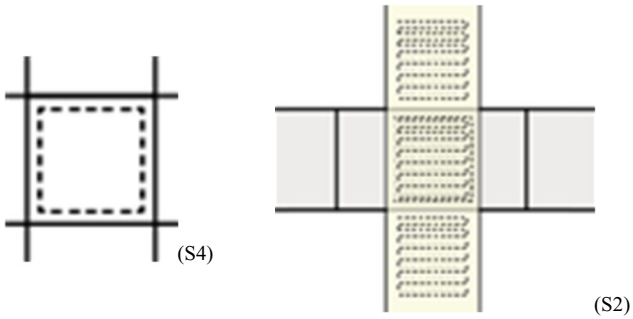


**Fig. 4** The two types of seams: (*S4*) and (*S2*)

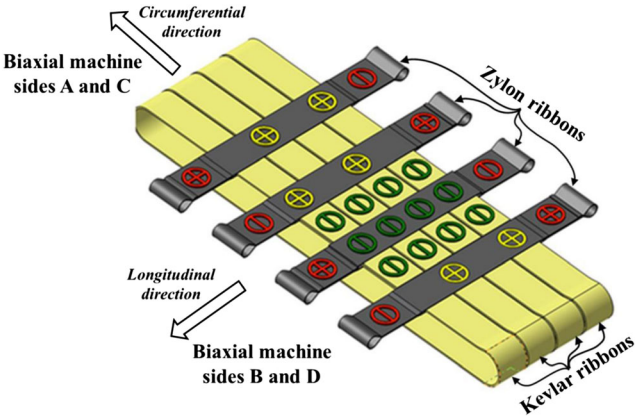


**Fig. 5** Restraint B/B: (sides *A* and *C*) Kevlar ribbons and (sides *B* and *D*) Zylon ribbons sewed with Nylon Zwibond 8 thread

two Zylon ribbons or three ribbons (two Zylon and one Kevlar) (⊕ in Fig. 5); S2 seam links two Kevlar ribbons or 4 ribbons (two Kevlar and two Zylon) (⊖ in Fig. 5).

## Experimental Setups

The biaxial tensile tests were performed using a home-design device equipped with twelve independent jacks along two orthogonal axes (Fig. 6). The jacks are place in between two stiff square steel frames and can slide on two rails, on each side, to permit the transversal displacements in the direction orthogonal to the load. The connection system of the jacks has a hinge allowing the correct alignment to the load direction. Each jack has a brushless motor equipped with an absolute encoder and coupled with a planetary gearbox to transform rotational into linear motion through a ball screw mounted on the axis. The maximum speed is 240 mm/min and the maximum stroke is 512 mm with a displacement accuracy of ± 0.05 mm. Two load cells are available for each jack with maximum nominal load of 15 and 50 kN. As consequence the maximum load for each side can be 45 and 150 kN.

Different clamping systems are available or can be adapted to the device. The clamping system adopted for the cruciform specimens consist of a pin and two shaped metallic plates (Fig. 7(a)). The arm of the specimen is wrapped on the pin and both are fixed between the two plates by two screws. Only for the Kevlar ribbon of specimens with seam S2, due to the expected higher load level, the two ends were folded and stitched to create buttonholes, avoiding sliding in the grips. The clamp system and the jack are connected with a hinge to have a correct alignment of the load and the arm.

A dedicated clamping system was designed and built for the Restraint B/B (Fig. 5) of the inflatable module of space habitats. The clamping of the Zylon ribbons consisted of a metallic pin (one on each side B and D in Fig. 7(b)) inserted in the three buttonholes of the ribbons and then clamped between two shaped plates with screws. The plates were screwed to a third component linked to three jacks by hinges.

Two metallic plates were placed in the closed rings of Kevlar ribbons (side A and C in Fig. 7(b)). Each plate is than fixed to a 'C' shape component connected to three jacks by hinges.

The biaxial tensile test of the Restraint B/B was assisted with a digital camera (Nikon D800) acquiring frames of the full sample at a frequency of 1 Hz with a resolution of 5520 × 3680 pixels. The images post-processing allowed the measurement of the full field displacement and the calculation

**Table 3** Parameters of seams S4 and S2

| | S4 | S2 |
|---|---|---|
| Pattern | Box | Ferrari |
| Thread | Nylon Zwibond 8 | Nylon Zwibond 8 |
| | (100 % Nylon 6.6 bonded Nm. 8 black) | (100 % Nylon 6.6 bonded Nm. 8 black) |
| Number of stitches | 103 | 303 |
| Stitch rate | 2 stitches/mm | 2 stitches/mm |
| Machine | Juki AMS-221E – campo | Juki AMS-221E – campo |
| | 800 × 400 | 800 × 400 |
| Needle | Model Groz-Beckert | Model Groz-Beckert |
| | Gebedur Nm 332/160-180 | Gebedur Nm 332/160-180 |
| Thread tension | 60–90 g | 90 g |

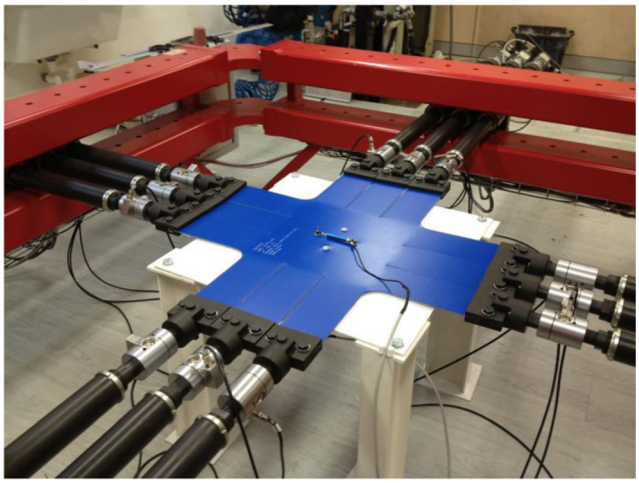

**Fig. 6** Biaxial tensile device

of strain on the external surface of the sample during loading by the digital image correlation (DIC) technique using the software Vic2D [8]. For this purpose, the surface of the sample was randomly speckled with white and black acrylic paints. DIC is a contactless technique which offers qualitative and quantitative information on the heterogeneous deformation of the sample surface [9]. It provides the full-field displacement and strain comparing images of the speckled surface before and after deformation. This technique was particularly suitable for the present biaxial tests for monitoring continuously the evolution of strain on the complete sample.

## Experimental Procedures

Biaxial tests of cruciform specimens (single intersection) aimed to verify the strength of both seams (S4 and S2). The applied biaxial loading does not refer to any international standard. The tests were conducted on three specimens for each seam, setting constant loads variation. The loading was supposed up to a predefined load level and, during the entire test, force of each load cell and stroke of each jack were recorded with a frequency of 1 Hz.

For sewing type S4, the adopted maximum load was 15 kN, as a limit to be verified in comparison of preliminary uniaxial test results, and the quasi-static loading speed was 500 N/s in both directions. Initial pre-tensioning, 110 N in both directions, was imposed to have the specimen in the loading plane.

For sewing type S2, the maximum load in the Kevlar ribbon direction was set to 41 kN, while 25 kN was for the Zylon one. These maximum loads in the both directions were set considering preliminary numerical analyses using the LS-Dyna™ software. The quasi-static loading speed was different in the two directions: 410 N/s for the Kevlar ribbon and 240 N/s for the Zylon one. This difference was set to reach simultaneously the imposed maximum loads. As for S4, initial pre-tensioning was imposed: 140 N on the Kevlar ribbon and 100 N the Zylon one.

During loading the specimen was regularly inspected (every 10 kN on Kevlar side) to detect visible imparted damages.

The purpose of the biaxial test of the Restraint B/B was to verify the behaviour and the structural integrity of the assembly. The test was conducted under biaxial load control up to predefined load resultants: 150 kN for the Kevlar ribbons direction and 80 kN for the Zylon one. These maximum loads in the both directions were set considering preliminary numerical analyses using the LS-Dyna™. The load rate for the two directions was: 167 and 100 N/s for Kevkar and Zylon ribbons direction, respectively. The load rates were selected to simulate the loading during air inflation in the module. Pre-tensioning of 300 N, in the both directions, was imposed before the beginning of the test. The pre-load was supposed to

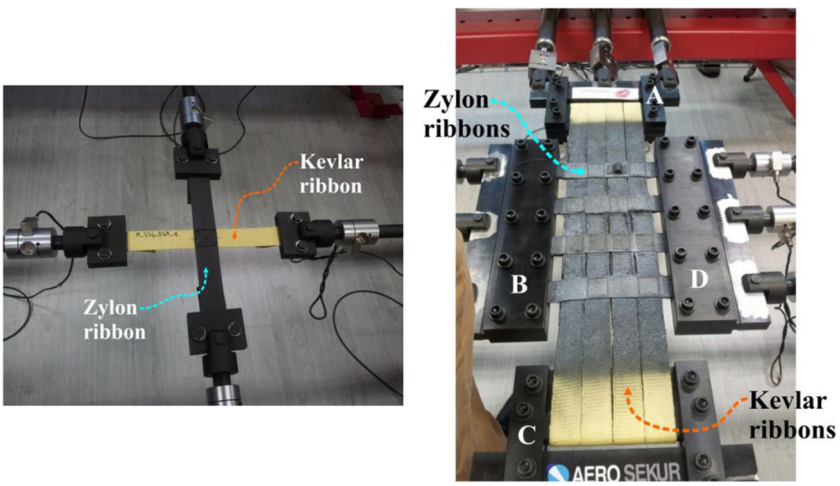


**Fig. 7** Clamping systems for: (**a**) cruciform specimens; (**b**) Restraint B/B

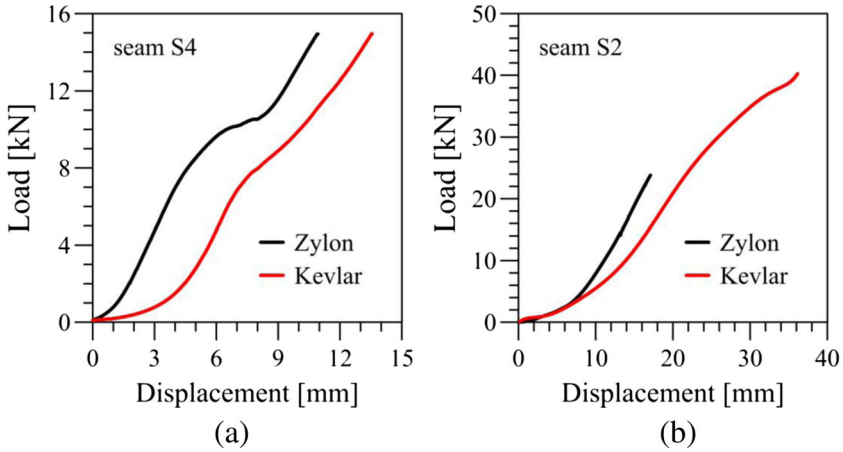


**Fig. 8** Typical load vs. displacement curve for the biaxial load of cruciform specimens with seam: (**a**) S4 and (**b**) S2

recover the possible small out of plane displacement that could affect the measurement of the displacement field by 2D DIC. An initial out of plane displacement can appear for de-crimp of the tows in the ribbons and flattening of the ribbons in the connection zones. Another source of out of plane displacement can be the transverse contraction during loading of the ribbons, but this can be considered negligible assuming the variation of thickness detailed in Tables 1 and 2.

The applied forces and the strokes of each jack were recorded with a frequency of 2 Hz.

During loading, the test was paused for 1 min every multiple of 10 kN to visually inspect the specimen status.

## Experimental Results

The first part of the experimental campaign was dedicated to the biaxial mechanical response of seam connections S2 and S4 (Fig. 4). Typical response of the two connections is summarized in Fig. 8. The curves detail the imposed load and the measured displacement for each load direction during the complete test. Two different behaviours were observed. After an initial alignment of the ribbons to the load direction, the seam S4 (low load bearing) had an almost constant stiffness of both ribbons up to a load level (≈8 kN) for which a reduction of the slope of the curves was observed more evident for the Zylon one (Fig. 8(a)). This is consequence of the damage imparted in the connection leading to a localized failure in the Zylon ribbon along one side of the stitching (Fig. 9(a)). The seam S2 (high load bearing) show a different mechanical performance than S2. The imposed biaxial loading gives the typical curves in Fig. 8(b). Only in the Kevlar direction an initiation of stiffness reduction was observed close to the maximum load, but damages were not visually detected (see the connection after the test in Fig. 9(b)). Therefore, it could be supposed an initiation of damage in the connection, not visible, that could lead to failure for a higher load level than the one considered.

The biaxial loading of the restrained B/B sample aimed to observe and measure the behaviour of the component during quasi-static loading as in a real inflatable module skin. The test is not intended for the investigation of the restrained B/B up to failure. The complete curves loads vs. displacements for each side are collected in Fig. 10. The first part of the curves shows negligible loads for increasing displacements as results of an initial adjustment of the sample to get the ribbons aligned with the loads directions. The continuous curves without abrupt variations

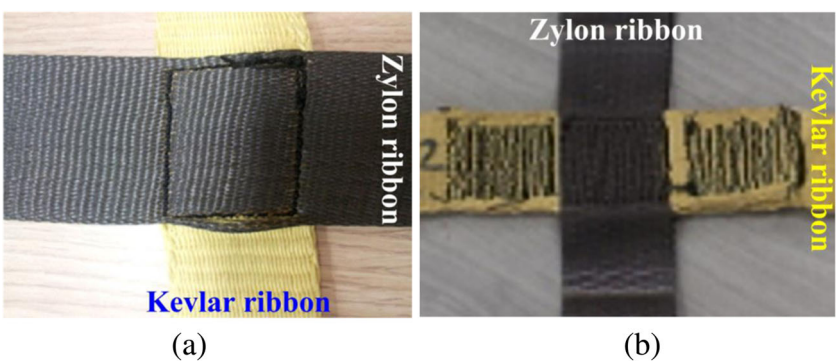


**Fig. 9** Damage after biaxial lading of the connection with seam (**a**) S4 and (**b**) S2

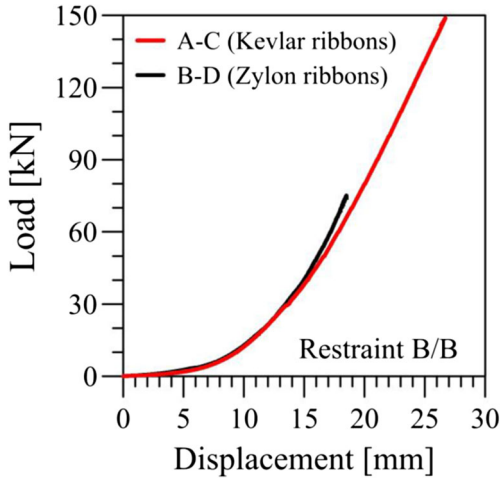


**Fig. 10** Load vs. displacement curve for the Restrained B/B sample

indicate absence of macro damages in the sample. This is confirmed observing with naked eyes the sample during the pauses of the loading, as mentioned above. No visible damages were detected during the complete loading history.

To better investigate and detect possible damages imparted, the strain maps were calculated for each acquired picture. The full field strain map on the surface of the sample during loading was calculated with the digital image correlation technique (DIC) implemented in the commercial software Vic2D [8]. Some of the adopted parameters were: subset size 40, step size 4, filter size 15. Those were selected considering that lower values of subset and step sizes did not generate considerable variation of the calculated strain filed. The strain maps cover the B/B sample excluding the external zones of the ribbons (see Fig. 11). This allows avoiding local problem in the images correlation due boundary effects and lack of speckle pattern on small parts of the sample at the intersection of the ribbons.

The distribution of the strain components in the main loading directions A-C and B-D are depicted in Fig. 11 at the maximum biaxial loading imposed. The local strain

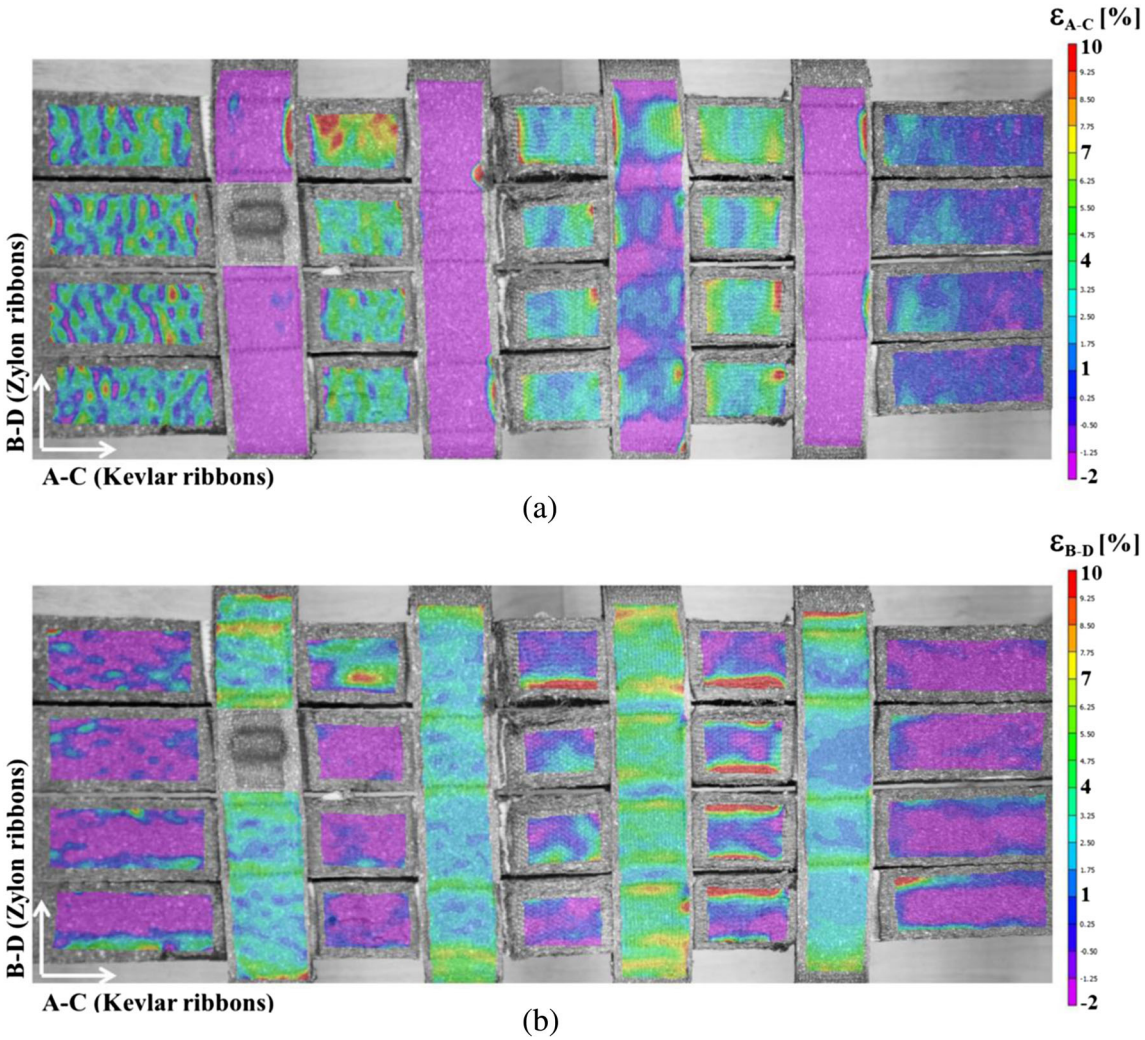


**Fig. 11** Contour plot of the strain components in direction (**a**) *A-C* and (**b**) *B-D* for a biaxial load of 148 kN and 75 kN in *A-C* and *B-D*, respectively

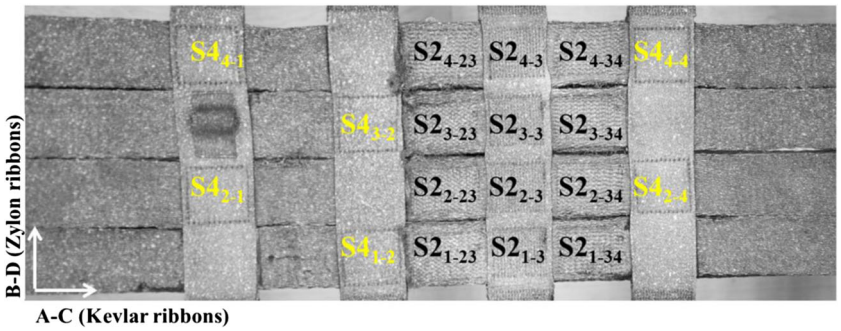


**Fig. 12** Identification of the connection zones for the load vs. average strain diagrams

distributions on the ribbon are almost similar in both directions, except some local concentration mainly close to the lateral boundaries of the ribbons. The same strain levels were recorded in both directions despite the different applied loads. This reveals a uniform deformation of the sample representing the restraint layer of an inflatable module skin, as expected in the design phase. Excluding the local concentration on the boundary of the ribbons, the sample did not have particular localization of deformation, meaning local damages were not detected on the observed external surface of the restrained B/B sample.

The evolution of the average strain components in the loading directions (Fig. 13) provides information on the behaviour of the connection zones of the restrained B/B sample. The nomenclature and position of the connection zones are detailed in Fig. 12. Assuming an increasing numbering of the Kevlar ribbons (direction A-C) from the bottom to top and of the Zylon ribbons (direction B-D) from the left to right, the zone $S4_{4-1}$ (sewing S4) is located at the connection of the forth line of Kevlar ribbons and the first line of Zylon ribbons; while, e.g., the zone $S2_{4-34}$ (sewing S2) indicates the connection of the forth line of Kevlar ribbons in between the third and fourth lines of Zylon ribbons.

Figure 13 shows the average, on the surface of some sewing, of the two strain components during the complete loading history. The level of the average strain in the direction A-C ($\varepsilon_{A\text{-}C}$) is higher, as expected, in the connection zones with Kevlar ribbons ($S2_{4-34}$) than in $S2_{4-3}$ where Kevlar and Zylon ribbons are sewed (Fig. 13(a)). This depends on the reduction of the strain component $\varepsilon_{A\text{-}C}$ in the connection $S2_{4-3}$ due to the contraction of the Zylon ribbons loaded in B-D direction. On the other hand, in the B-D direction, the highest strain level ($\varepsilon_{B\text{-}D}$) is in $S2_{4-3}$, while, as expected, the connections of Kevlar ribbons (e.g. $S2_{4-34}$) increase slightly the width as consequence of the tension in the Zylon ribbons and the contraction of the Kevlar ones (Fig. 13(b)). Comparing the performance of the two different sewing S2 and S4 loaded in the direction B-D (see $S2_{4-3}$ and $S4_{4-1}$ in Fig. 12), they show a similar behaviour with a strain at the maximum load of 7 % higher for S2. This increase of deformation could depend on the higher number of stitches in S2 leading to a higher level of local misalignment of the threads in the ribbons recovered during loading. But, this could also be considered in a reasonable experimental scatter not measurable with the limited number of tests in the present investigation.

The diagrams in Fig. 13 show strain levels at the maximum biaxial loading close to the failure strain recorded for the ribbons (see Figs. 2 and 3). As observed above, the biaxial loading of the restrained B/B did not lead to failure of the sample and no visible damages have been detected. Therefore, the strain levels recorded with the DIC technique are

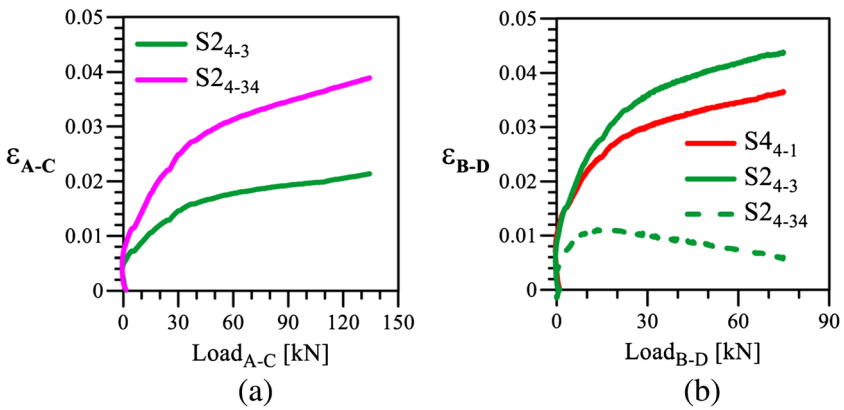


**Fig. 13** Load vs. average strain components in some connection zones of the Restrained B/B. (**a**) *A-C* (Kevlar ribbons) and (**b**) *B-D* (Zylon ribbons) direction

consequences of the different seam connections and the local alignment in the load direction of the threads deformed during stitching.

## Conclusions

The biaxial tensile behaviour of a representative breadboard segment of the structural restraint layer in an inflatable module for orbital and planetary space habitats was experimentally investigated. The sample contains perpendicular ribbons of two different materials connected with two different configurations of seam.

The extremely positive performance of the breadboard segment, measured with the biaxial loading and the full field strain recordings by the digital image correlation techniques, can be summarized, for the considered loads range representative of the real load conditions, considering that:

- the sample did not show visible initiation of macro damages during the complete biaxial loading history;
- despite the different applied loads, the distribution of the strain components in the main loading directions highlights almost similar levels in the perpendicular ribbons, this reveals a uniform deformation of the sample as supposed in the design phase;
- excluding some local concentrations on the boundary of the ribbons, the sample did not show localization of deformation, meaning absence of local damages.

Similar mechanical details, as reported in this experimental activity, are, in the authors' knowledge, not easily available in the literature. Therefore, they can help to increase the confidence on future developments of advance light inflatable moduli for space habitats.

**Acknowledgments** The activities were performed within the STEPS2 Project (Systems and Technologies for Space Exploration phase 2). STEPS2 is a project co-funded by European Union within the platform "Misura Piattaforme Innovative" - Phase 2 of POR FESR 2007/2013.

The Textiles HUB (Heuristic Understanding in Buildings) laboratory at "Politecnico di Milano" is gratefully acknowledged for the experimental devices adopted in this work.

## References

1. Nebiolo M (2013) Inflatable modules in space
2. Mileti S, Guarrera G, Marchetti M, Ferrari G, Nebiolo M, Augello G (2006) The FLECS expandable module concept for future space missions and an overall description on the material validation. Acta Astronaut 7
3. Nebiolo M, Palmieri P, Manfredi L, Augello G, Langlois S (2008 Design & manufacturing of a subscale inflatable module (IMOD) for manned space applications – ESA TRP. In: Proceedings of the 4th European Workshop on Inflatable Space Structures, Noordwijk
4. Nebiolo M, Palmieri P, Gomiero F, Pirolli M, Langlois S (2011) Inflatable technology for manned space applications: the IMOD experience. In: Proceedings of the 5th European Workshop on Inflatable Space Structures, Noordwijk
5. Inflatable Material for Space Final. STEC contract 16937/03/NL/MV
6. TN2 – Materials and Materials Configurations for the Walls of an Inflatable Module. IMOD Program, IHAB-ALS-TNO-0009
7. www.chemours.com/Viton/en_US/, [Online]
8. Correlated Solutions, Inc. (2012) VIC-2D, Irmo. http://www.correlatedsolutions.com
9. Sutton MA, Orteu JJ, Shreir HW (2009) Image correlation for shape, motion and deformation measurements: basic concepts, theory and applications. Springer Science